Methodology for the Diagnosis of Hydromechanical Actuation Loops in Aircraft Engines

Benjamin Lamoureux[1,2], Jean-Rémi Massé[3], and Nazih Mechbal[4]

[1,3]*Snecma (SAFRAN Group), Systems Division, Villaroche, France*

benjamin.lamoureux@snecma.fr, jean-remi.masse@snecma.fr

[2,4] *Arts et Métiers ParisTech, PIMM, Paris, France*

nazih.MECHBAL@ensam.eu

***Abstract*— This document provides a method for on-board monitoring and on-ground diagnosis of a hydromechanical actuation loop such as those found in aircraft engines. First, a complete system analysis is performed to understand its behaviour and determine the main degradation modes. Then, system health indicators are defined and a method for their real time on-board extraction is addressed. Diagnosis is performed on-ground through classification of degradation signatures. To parameterize on-ground treatment, both a reference healthy state of indicators and degradations signatures are needed. The healthy distribution of indicators is obtained from data and a physics-based model is used to simulate degradations, quantify indicators sensibility and construct the signatures database. At last, algorithms are deployed and a statistical validation of the performances is conducted.**

I. INTRODUCTION

In aircraft engine industry, one of the greatest challenges is to increase products availability because costs of ownership induce prohibitive expense during aircraft immobilization. Up to now, delays and cancellations occurred randomly because system component failures were not predictable. Nowadays, new means of computation makes it possible to monitor the evolution of many engine's features and prognostics and health management (PHM) [1] has become not only a possibility but a necessity to anticipate unwanted events. For aircraft engine manufacturers, PHM is a double challenge: to limit delays and cancellations and to reduce the time of maintenance operations by providing operators with trouble shooting assistance.

A good summary of the main works done in the PHM field can be found in [2] and some of the methods have already been experimented in particular in the field of electronics, for example to monitor the remaining useful lifetime of batteries [3]. In France, some works such as [4] or [5] have addressed the issue of modelling a multi-levels architecture for a complex system's monitoring process or formalizing the prognostics process [6].

As far as predictive monitoring applied to aeronautics is concerned, research is focused on developing mathematical tools for diagnosis and prognostics [7]. Some good reviews on the subject can be found in [8] for the diagnosis and [9] for prognostics.

However, academic research and industrial needs are not on the same page on the following points: (1) experimental studies are restricted to sensor faults, vibration analysis and structural health monitoring (SHM) [10] but health assessment of control systems is rarely addressed; (2) papers commonly make the hypothesis that every variable is measured so indicators are easily constructible but actually, position, number and precision of sensors is defined and most of the time not modifiable; (3) because of data storage issues, indicators extraction must be performed on-board and the specific constraints related to the real time in-situ computation is almost never addressed and (4) physics-based models are necessary to quantify the impacts of degradation and their potential evolution.

This document focuses on the diagnosis of the following system: an actuation loop which purpose is to regulate the position of an aircraft engine variable geometry. The study will be articulated around five points: System Analysis, Indicators Definition, Degradations Modelling, Indicator Transformation Laws Computation and Statistical Validation of Performances.

II. SYSTEM ANALYSIS

In order to monitor a system, the first step is to determine its degradation modes and it can be achieved through expertise, experience feedback or Failure Mode and Effects Analysis (**FMEA**).

The system is a closed loop composed of three main components: A controller, a servovalve and a cylinder. The position of the cylinder is measured by a linear variable differential transformer (**LVDT**), as shown in Fig. 1. The controller is of type proportional–integral–derivative (**PID**).

This study will focus on the mechanical degradations of the system and electrical ones will not be treated. For example, electrical wires oxidation, micro cuts and connectors' faults will not be addressed.

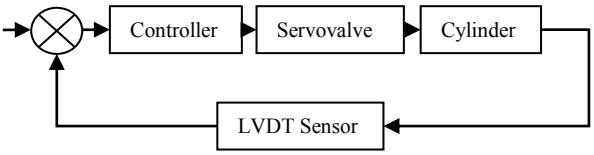

Fig. 1 : Schematic of the hydromechanical actuation loop

A. Degradation modes of a servovalve

In this application, the studied servovalve type is two-stage flapper-nozzle. In this type of servovalve, the power transmission chain is the following one:

1. A control current is send to a torque motor
2. The current is converted to a displacement of the flapper through an electromagnetic effect
3. The displacement of the flapper changes the position of the second stage spool via a hydraulic control and
4. The position of the spool reorganizes the distribution of the flows. A flapper-nozzle servovalve configuration is shown in Fig. 2.

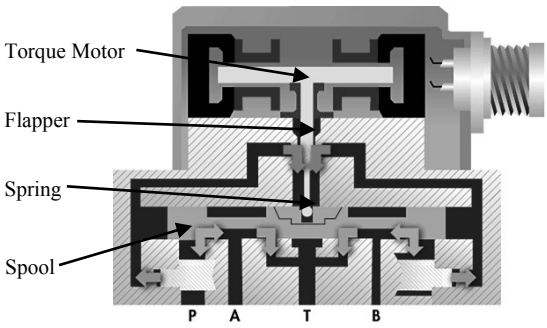

Fig. 2: Electrohydraulic flapper-nozzle servovalve configuration

The following list of the degradation modes selected for the servovalve is inspired by [11]:

1) Increased contamination of the filters: As dust and debris accumulate in the servovalve, filters gradually lose their efficiency and the hydraulic resistance increases. The result is a slower response of the servovalve.

2) Drift of the null bias current: As the torque motor ages and loses his magnetic properties, the null bias current of the servovalve, namely the current for which the flows are equal in control ports 1 and 2, can drift from its nominal value.

3) Increased backlash: With the progressive wear of the internal feedback spring, the hysteresis of the servovalve increases.

4) Increase of the friction force between spool and sleeve: This phenomenon is due to the cumulative effects of continuous movement of the spool and contamination of the hydraulic fluid because the debris induces a silting effect.

5) Increase in the radial clearance between spool and sleeve: Because of the contamination, abrasion of the corners of the spool lands resulting in an increase of internal leakage.

B. Degradation modes of a cylinder

The cylinder considered in this application is a double-acting hydraulic cylinder with a cooling diaphragm between the two sides. The hydraulic fluid used is fuel.

The following list of the degradation modes selected for the hydraulic cylinder is inspired by [12]:

1) Internal leakage between the two sides: As the seal ages, dust and debris accumulate between the seal and the sleeve resulting in an abrasive effect degrading the cylinder body.

2) Clogging of the cooling diaphragm: With the increase of the temperature, a coking of the fuel can occur, resulting in the clogging of the diaphragm.

C. Other potential degradation modes

The list of degradation modes presented above is not exhaustive and many other phenomenons can occur such as a damage of the kinematic chain downstream of the cylinder or the burst of a pipe but the choice was made to focus only on the servovalve and cylinder's degradations.

III. INDICATORS

A. Flow Gain curve of a Servovalve

Among the different measures characterizing a servovalve, the flow gain curve is one of the most significative because it displays both static and dynamic features as shown in Fig. 3.

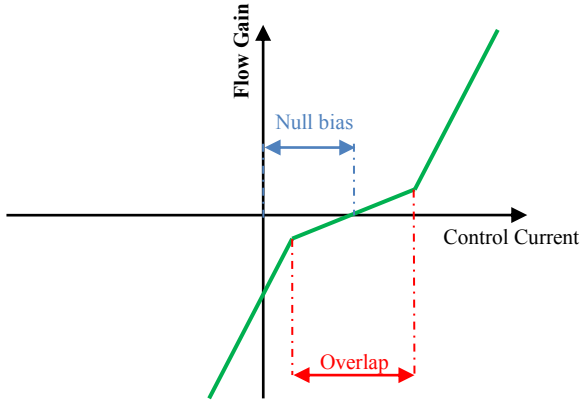

Fig. 3 : Flow Gain curve and main features

The extraction of this curve requires that the servovalve is equipped with flowmeters but in our application, only the position of the cylinder is measured. However, the cylinder's velocity V_{cyl} and the servovalve output flows in each control port Q_{SV_head} and Q_{SV_rod} can be linked via the simplified equation:

$$V_{cyl} = \begin{cases} (Q_{SV\_head} - Q_{cooling}) \,/S_{head} & \text{during shaft outlet} \\ -(Q_{SV\_rod} - Q_{cooling}) \,/S_{rod} & \text{during shaft inlet} \end{cases} \quad (1)$$

Where $Q_{cooling}$ is the cooling flow between the two sides of the cylinder and S_{head} and S_{rod} are respectively the cross-sectional area of the head and the rod sides.

B. *Velocity Gain of a hydromechanical loop*

In order to get around the lack of flowmeters to monitor the servovalve only, the idea is to monitor the whole loop by following salient features on the Velocity Gain curve.

This curve can be obtained only with the measures of both the control current $I_{control}$ and the cylinder's velocity V_{cyl}. The value of V_{cyl} is computed by derivation of the cylinder's position X_{cyl}.

Blue points in Fig. 4 are the result of an extraction of the velocity gain curve performed during an entire flight. Because of the hysteresis of the servovalve, the dispersion of the points is substantial and therefore a smoothing algorithm based on local means is applied to the data.

The curve smoothing is performed on-board through a real-time algorithm in order to store the least possible data in the controller during the flight. Then the on-ground part consists in processing the information contained in the curve and carrying out the health monitoring procedure.

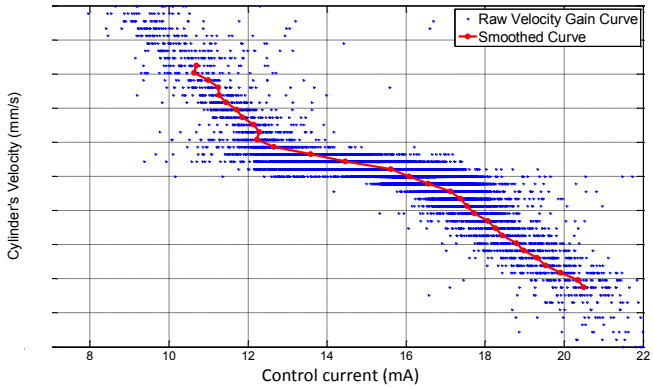

Fig. 4 : In-Flight extracted curve before and after smoothing

C. *Indicators Construction*

From the extracted curve, we define many indicators related to the targeted degradation. Those indicators are listed in Table I and their graphical equivalent is shown in Fig. 5.

TABLE I
INDICATORS EXTRACTED FROM THE CURVE

Names		**Targeted degradations**
Long	Short	
Slope change #1 abscissa	X_1	Degradations impacting the horizontal position of the curve → Increase of the radial clearance between spool and sleeve
Slope change #1 ordinate	Y_1	Degradations impacting the vertical position of the curve → Diaphragm clogging, cylinder internal leakage
Slope change #2 abscissa	X_2	Idem X_1
Slope change #2 ordinate	Y_2	Idem Y_1
Null Bias Current $I_{nb} = \frac{X_1 + X_2}{2}$	I_{nb}	Degradations impacting the value of the Null Bias → Null Bias current shift
Idle Current of the Loop (Current for null velocity)	I_0	Degradations impacting the static behaviour of the loop → All the degradations
Standard Deviation (hysteresis) at idle current	Hys_0	Degradations impacting the hysteresis → Increased Backlash
Velocity Gain for Shaft Inlet	G_{in}	Degradations impacting the global dynamic behaviour of the loop → Increased Backlash, Contamination of the filters, Increased friction force
Velocity Gain for Shaft Outlet	G_{out}	Idem G_{in}
Velocity Gain for Null Region	G_{null}	Idem G_{in}

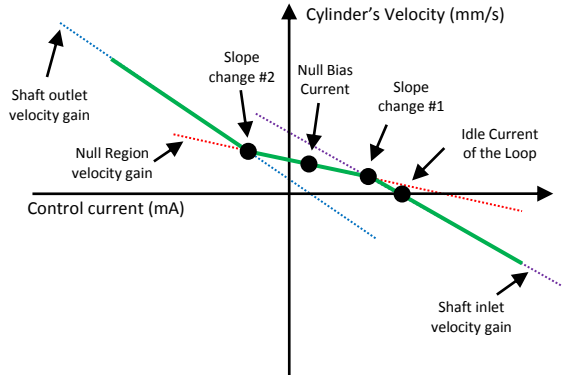

Fig. 5 : Graphical representation of the indicators

IV. DEGRADATIONS MODELING

A. *Model and Sub-models Construction*

A physical model of the hydromechanical system has been developed in Matlab-Simulink® in order to simulate its behaviour in presence of some degradation and to quantify their impacts. This model is composed of three sub-models: Servovalve, cylinder and controller. The granularity of the sub-models must be important enough to simulate all the degradations discussed in the system analysis. For example, the sub-model of the servovalve, the most complex one, must include the modelling of the two-stages, the filters and the feedback spring. A good method for modelling servovalves is given in [13].

There are two ways degradations can be modelled: additive and multiplicative. The former consists in adding a value to some variables and the latter consists in a multiplication of some variables as shown in **Erreur ! Source du renvoi introuvable.**. In **Erreur ! Source du renvoi introuvable.**, Y_u and U are healthy values of variables, f is the degradation intensity and Y is the degraded value of variables.

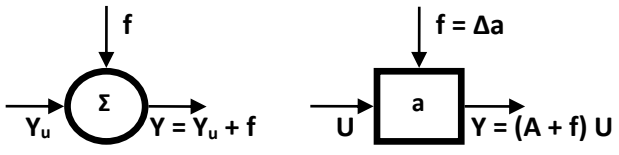

Fig. 6 : Additive and Multiplicative modelling of degradations

TABLE II
MODELLING OF DEGRADATIONS

Degradation	Modelling
Increased contamination of the filters	Multiplicative: To simulate a decrease of the efficiency, the flow is multiplied by a scalar in the range [0,1]
Drift of the null bias current	Additive: A value corresponding to the opposite of the drift is added to the control current.
Increased Backlash	Multiplicative: Modification of the transfer function governing the position of the spool in the second stage.
Increase of the friction force	Additive: Increase of the coefficient of friction between spool and sleeve.
Increase in the radial clearance	Multiplicative: Decrease of the restriction coefficient at the corners of the spool lands victims of abrasion.
Internal leakage between the two sides	Multiplicative: Increase of the restriction coefficient of the cooling flow
Clogging of the cooling diaphragm	Multiplicative: Decrease of the restriction coefficient of the cooling flow

B. Model Updating

The main hypothesis of this method is that operational data are available. Thus, it is supposed that the distribution of the indicators corresponding to a healthy state is well known.

For each simulation, the goal is to compute the velocity gain of the system by simulating the velocity of the cylinder for a gradually increasing control current from lower saturation boundary to upper saturation boundary.

Before simulating the degraded states, it is necessary to simulate and update the model parameters against operational data for the reference healthy state. Fig. 7 shows both extracted and estimated velocity gain curves for the healthy state. The estimated one is obtained from a model configured with averaged parameters given by constructors.

The result after model updating on parameters is also given in Fig. 7, and it can be noted that a difference remains between the curves around the idle current of the loop. The model used in this application is not enough accurate to explain this local deviation.

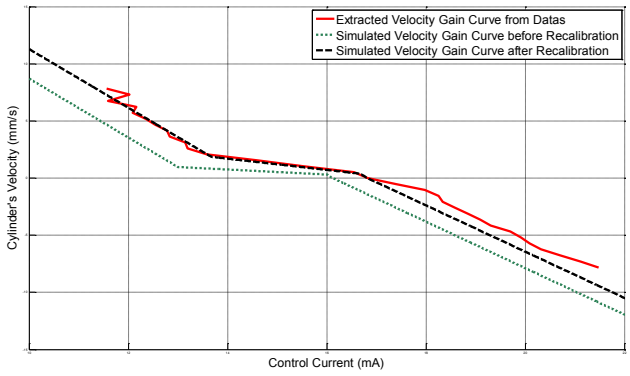

Fig. 7 : Extracted against Estimated Velocity Gain of the healthy state

C. Simulation of the degradations

For this paper, the focus will be on only two degradations namely the drift of the null bias current of the servovalve and the internal leakage between the two sides of the cylinder.

Results of the simulation on the updated model with those two degradations are given in Fig. 8.

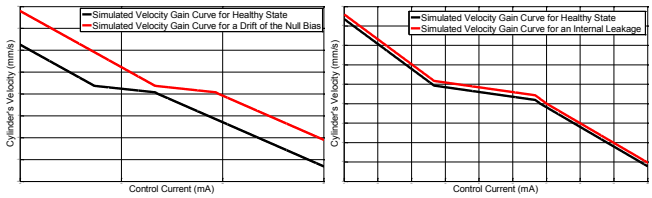

Fig. 8 : (a) Left: effect of a null bias drift. (b) Right: effect of an internal leakage in the cylinder

V. INDICATORS TRANSFORMATION LAW COMPUTATION

A. Construction of the laws

In this part, a design of experiment is generated to organize the simulations of the behaviour of the system in presence of degradations. For each case, simulations are run for gradually increasing intensities of degradation. Eventually, the results are summarized in the form of indicators transformation laws (**ITL**).

With Ind_i representing the i^{th} indicator in a healthy state, Ind_i^{deg} the i^{th} indicator in presence of the degradation deg, and Int^{deg} the intensity of the degradation deg, the ITL named F_i^{deg} corresponding to the i^{th} indicator and the degradation deg can be defined as follows:

$$Int^{deg} \xrightarrow{F_i^{deg}} \Delta I_i^{deg} = A_i^{deg} \times Int^{deg} \quad (2)$$

Where A_i^{deg} is the coefficient of the linear regression of ΔI_i^{deg} with respect to Int^{deg}. ΔI_i^{deg} is the change in the value of the indicator and can be also expressed this way:

$$\Delta I_i^{deg} = Ind_i^{deg} - Ind_i \quad (3)$$

Thus, F_i^{deg} provides the change in the indicator's value for a given intensity of degradation.

B. Utilization of the laws

Once computed, an ITL makes it possible to generate an estimated value of indicators for a degraded state from a healthy value computed from operational data according to the following equation:

$$I_i^{deg} = I_i^{healthy} + \Delta I_i^{deg} \quad (4)$$

In this application, 7 degradations and 10 indicators are considered, which means that 70 ITL must be computed. For instance, the law giving the value of X_1 for the degradation drift of the null bias current is:

$$I_{X1}^{NB\ drift} = I_{X1}^{healthy} + A_{X1}^{NB\ drift} \times Int^{NB\ drift} \quad (5)$$

Where $I_{X1}^{healthy}$ is computed by averaging the extracted value of X_1 for a given number of flights for which the system is considered flawless.

VI. STATISTICAL VALIDATION OF PERFORMANCES

A. Key Performance Indicators

For this application, both fault detection and diagnosis are addressed. A presentation and definition of Key Performance Indicators (KPI) is given in Table III.

TABLE III
KEY PERFORMANCE INDICATORS

KPI	Definition
False Positive Rate	Proportion of False Positive (false alarm) among all the states where a fault is detected
False Negative Rate	Proportion of False Negative (undetected faults) among all the states where no fault is detected
False Classification Rate	Proportion of False Classification among all classifications
Robustness	Capacity of the monitoring system to be still efficient when some parameters drift from their nominal values.

B. Method for fault detection and diagnosis

A more precise presentation of the method presented below can be found in [14].

1) Indicators Model Learning:

The first step is to learn a Gaussian model of the indicators distribution in a reference state, typically a healthy state. The model is learned from extracted indicators on a given number of flights and is presented as follows:

$$Model(i) = \begin{pmatrix} \mu_i^{healthy} \\ \sigma_i^{healthy} \end{pmatrix} \quad (6)$$

Where $\mu_i^{healthy}$ is the mean of the indicators and $\sigma_i^{healthy}$ their standard deviation.

2) Fault Detection:

It is based on an abnormality score named Z_{score}. For the indicator i, $Z_{score,i}$ is defined as follows:

$$Z_{score,i} = \frac{I_i - \mu_i^{healthy}}{\sigma_i^{healthy}} \quad (7)$$

Where I_i is the currently measured value of indicator.

Then a global abnormality score of the system $Global\_Z_{score}$ is computed from $Z_{score,i}$ with $i \in [1; 10]$ via the Mahalanobis distance [15].

Indicators are extracted on-board and $Global\_Z_{score}$ is computed on-ground at each flight. The parameterization of the fault detection consists in defining a relevant threshold value Thr and if the value of $Global\_Z_{score}$ crosses Thr, it means that a fault has been detected.

3) Diagnosis:

Diagnosis is performed via a classification of signatures. A signature is a vector of indicators. For this application, a signature is a vector appending 10 indicators extracted from flight data:

$$Sign = \left(Z_{score,X_1}, Z_{score,Y_1}, \dots, Z_{score,G_{null}}\right)^T \quad (8)$$

If the system is healthy, $Sign$ is a zero vector of size 10.

Assuming that the maximal intensities of the degradations are known, it is possible to determine the signatures of the degradations $Sign_{ref,deg}$ associated.

$$Sign_{ref,deg} = \left(\frac{I_{X_1}^{deg} - \mu_{X_1}^{healthy}}{\sigma_{X_1}^{healthy}}, \dots, \frac{I_{G_{null}}^{deg} - \mu_{G_{null}}^{healthy}}{\sigma_{G_{null}}^{healthy}}\right)^T \quad (9)$$

When a fault is detected, the classification algorithm is run. This algorithm is based on a pattern recognition method which finds the reference signature that most closely matches the currently measured signature. A guilt probability is assigned to each component of the system.

C. Statistical Validation

1) Matrix of the signatures

To perform fault detection and diagnosis, it is essential to determine the matrix of the signatures. It shows the signature corresponding to the maximal intensity of the degradations. A part of this matrix, taking into account only two degradations is given in Table IV.

TABLE IV
MATRIX OF THE SIGNATURES

Degradation	Influences (Z_{scores})									
	X_1	Y_1	X_2	Y_2	I_{nb}	I_0	Hys_0	G_{in}	G_{out}	G_{null}
Drift of the null bias current	24	0	26	0	28	24	0	0	0	0
Internal leakage between the two sides	0	4	0	11	0	1	0	0	0	0

2) Performances of fault detection

Once the matrix of the signatures is available, a detection threshold Thr on the global score $Global\_Z_{score}$ must be defined.

The value of this threshold must be low enough to ensure detection of all the different degradation, even those not provided by the system analysis and high enough to ensure a low rate of false alarms. To set this value in an optimal way, it is essential to take into account the standard deviation of the $Global\_Z_{score}$.

First, the computation of the probability density function of $Global\_Z_{score-healthy}$ is performed to set a first value of Thr, as shown in Fig. 9. Typically, the chosen value for Thr is:

$$Thr = \mu_{healthy} + A \times \sigma_{healthy} \quad (10)$$

At first approach, the chosen value for A is $A = 2$ because it ensures that only 5% of false detection. However, this value can potentially limit the false negative rate so it is necessary to check if the degradations are still detectable.

To ensure the performances, the distributions of $Global\_Z_{score-healthy}$, $Global\_Z_{score-leak}$ and $Global\_Z_{score-drift}$ are compared as presented in Fig. 9.

Performances for different values of *A* are presented in Table V.

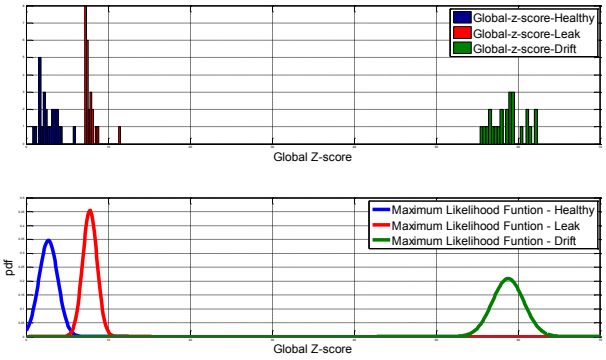

Fig. 9 : Distribution of Global_scores and likelihood functions

TABLE V
FAULT DETECTION PERFORMANCES

A	Null Bias Drift		Internal Leakage	
	False Positive	False Negative	False Positive	False Negative
0	0%	0%	50%	0%
1	0%	0%	16%	0%
2	0%	0%	3%	0%
3	0%	0%	0.3%	2%

3) Performances of diagnosis

The classification algorithm gives, for each component of the system, a probability of guilt proportional to the colinearity between the current signature and the referenced signatures. The diagnosis performances depend on the intensity of the degradations. Results are shown in Table VI.

TABLE VI
DIAGNOSIS PERFORMANCES

Effective Degradation	Percentage of max intensity (From ITL)	Probability of guilt of Drift	Probability of guilt of Leak
Drift	25%	0.94	0.06
Drift	50%	0.94	0.06
Drift	100%	0.94	0.06
Leak	25%	0.37	0.63
Leak	50%	0.13	0.87
Leak	100%	0.11	0.89

VII. CONCLUSION

This paper provides a methodology to perform fault detection and diagnosis on a hydromechanical actuation loop. A first part details how to construct relevant indicators to perform on-board extraction of indicators and a second part how to achieve and validate fault detection and diagnosis on-ground. It must be noted that further works will follow, dealing with the management of uncertainties, the architecture of monitoring for a wider system and also prognostics.

REFERENCES

[1] J. Sheppard, M. Kaufman et T. Wilmer, «IEEE Standards for Prognostics and Health Management,» *Aerospace and Electronic Systems Magazine,* vol. 24, n° %19, p. 34–41, 2009.

[2] A. Jardine, D. Lin et D. Banjevic, «A review on machinery diagnosis and prognostics implementing condition-based maintenance,» *Mechanical systems and signal processing,* vol. 20, n° %17, p. 1483–1510, 2006.

[3] B. Saha et K. Goebel, «Uncertainty management for diagnosis and prognostics of batteries using Bayesian techniques,» chez *IEEE Aerospace Conference*, Big Sky, 2008.

[4] A. Muller, Contribution à la maintenance prévisionnelle des systèmes de production par la formalisation d'un processus de pronostic, PhD thesis from the Nancy I University - Henri Poincaré, 2005.

[5] P. Ribot, Vers l'intégration diagnostic-pronostic pour la maintenance des systèmes complexes, PhD thesis from the Toulouse III University - Paul Sabatier, 2009.

[6] P. Cocheteux, Contribution à la maintenance proactive par la formalisation du processus de pronostic des performances de systèmes industriels, PhD thesis from the Nancy I University - Henri Poincaré, 2010.

[7] J. Massé, B. Lamoureux and X. Boulet, "Prognosis and Health Management in system design," in *IEEE International Conference on Prognostics and Health Management*, Denver, 2011.

[8] A. Patterson-Hine, G. Biswas, G. Aaseng, S. Narasimhan et K. Pattipati, «A Review of Diagnostic Techniques for ISHM Applications,» vol. 1st Integrated Systems Health Engineering and Management Forum, 2005.

[9] M. Roemer, C. S. Byington, G. Kacprzynski et G. Vachtsevanos, «An overview of selected prognostic technologies with application to engine health management,» chez *Proceedings of GT2006 ASME Turbo Expo* , Barcelona, 2006.

[10] N. Mechbal, M. Vergé, G. Coffignal and M. Ganapathi, "Application of a combined active control and fault detection scheme to an active composite flexible structure," *Mechatronics vol. 16,* pp. 193-208, 2006.

[11] L. Borello, M. D. Vedova, G. Jacazio et M. Sorli, «A Prognostic Model for Electrohydraulic Servovalves,» *Annual Conference of the Prognostics and Health Management Society,* 2009.

[12] P.-Y. Crepin et R. Kress, «Model Based Fault Detection for an Aircraft Actuator,» chez *22nd Congress of International Council of the Aeronautical Sciences*, Harrogate, 2000.

[13] B. Attar, Modélisation réaliste en conditions extrêmes des servovalves électrohydrauliques utilisées pour le guidage et la navigation aéronautique et spatiale, Thèse de l'Université de Toulouse, délivré par l'INSA de Toulouse, 2008.

[14] J. Lacaille, «Standardized failure signature for a turbofan engine,» chez *Aerospace conference, 2009 IEEE* , Big Sky, MT, 2009.

[15] R. De Maesschalck, D. Jouan-Rimbaud et D. Massart, «The mahalanobis distance,» *Chemometrics and Intelligent Laboratory Systems,* vol. 50, n° %11, pp. 1-18, 2000.